# Data-driven time-frequency analysis of seismic data using non-stationary Prony method[a]

[a]Published in Geophysical Prospecting, 66, 85-97 (2018)

*Guoning Wu*, Sergey Fomel†, Yangkang Chen‡*

## ABSTRACT

The empirical mode decomposition aims to decompose the input signal into a small number of components named intrinsic mode functions with slowly varying amplitudes and frequencies. In spite of its simplicity and usefulness, however, the empirical mode decomposition lack solid mathematical foundation. In this paper, we describe a method to extract the intrinsic mode functions of the input signal using non-stationary Prony method. The proposed method captures the philosophy of the empirical mode decomposition, but use a different method to compute the intrinsic mode functions. Having the intrinsic mode functions obtained, we then compute the spectrum of the input signal using Hilbert transform. Synthetic and field data validate the proposed method can correctly compute the spectrum of the input signal, and could be used in seismic data analysis to facilitate interpretation.

## INTRODUCTION

Time-frequency analysis maps an 1D time signal into 2D time and frequency domains, which can capture the non-stationary character of seismic data. Time-frequency analysis is a fundamental tool for seismic data analysis and geological interpretation (Castagna et al., 2003; Reine et al., 2009; Chen et al., 2014; Liu et al., 2016). Conventional time-frequency methods, such as short time Fourier transform (Cohen, 1989), wavelet transform (Mallat, 1989) and S-transform (Stockwell et al., 1996) are under the control of Heisenberg/Gabor uncertainty principle, which states that we cannot have the energy arbitrarily located in both time and frequency domains (Mallat, 2009). Moreover, short time Fourier transform, wavelet transform and S-transform are using a windowing process, which often brings smearing and leakage (Tary et al., 2014). Therefore spurious frequencies are often generated, which will "color" the real time-frequency map and affects the interpretation. In recent years, many new methods were proposed such as matching pursuit (Mallat and Zhang, 1993), basis pursuit (Chen et al., 1998), empirical mode decomposition (Huang et al., 1998; Chen and Fomel, 2015), the synchrosqueezing wavelet transform (Daubechies et al., 2011) and its variants such as the synchrosqueezing short time Fourier transform (Oberlin et al., 2014), the synchrosqueezing S-transform (Huang et al., 2015). The matching

pursuit and basis pursuit methods represent the energies of the input signal by the energies of atoms found using different methods, which prevents smearing and leakage, creating highly localized time-frequency decompositions. The efficiency of these two methods depend on the predefined dictionary (Tary et al., 2014). The empirical mode decomposition method decomposes a signal into symmetric, narrow-band waveforms named intrinsic mode functions to compress artificial spectra caused by sudden changes and to therefore improve the time-frequency resolution (Han and van der Baan, 2013). However, the empirical mode decomposition also suffers from mode mixing and splitting problems. In order to solve the above problems, alternative methods were developed based on empirical mode decomposition: ensemble empirical mode decomposition(Wu and Huang, 2009), complete ensemble empirical mode decomposition (Torres et al., 2011). However, these two methods, like the empirical mode decomposition, are still "empirical" because their sketchy mathematical justifications. The synchrosqueezing wavelet transform (Daubechies et al., 2011) and its variants capture the philosophy of empirical mode decomposition, but use a different method to compute the intrinsic mode functions providing a rigorous mathematical framework.

Similar to the Fourier transform, the Prony method (Prony, 1795) decomposes a signal into a series of damped exponentials or sinusoids in a data-driven manner, which allows for the estimation of frequencies, amplitudes, phases and damping components of a signal. Fomel (2013) proposed the non-stationary Prony method (NPM) based on regularized non-stationary auto-regression. The NPM decomposes a signal into intrinsic mode functions with controlled smoothness of amplitudes and frequencies like the empirical mode decomposition does, but uses NPM instead. Unlike Fourier transform, the coefficients of the extracted intrinsic mode functions for the Prony method do not clearly define the energy distribution for the input signal in the time-frequency domain. Therefore, the NPM used by Fomel does not clearly define a "real" time-frequency map but a "time-component" map. In this paper, we couple the NPM (Fomel, 2013) and the Hilbert transform to give a time-frequency decomposition. The proposed method has a rigorous mathematical framework. Furthermore, synthetic and real data tests confirm that the intrinsic mode functions derived by the proposed method are more smooth with respect to the amplitudes and frequencies than the intrinsic mode functions of ensemble empirical mode decomposition (Wu and Huang, 2009). Synthetic and real data tests also confirm that the proposed method has a higher time-frequency resolution than the ensemble empirical mode decomposition. The proposed method can be used to facilitate seismic interpretation.

## THEORY

We give a short description of the theories for empirical mode decomposition, Prony, and NPM. For details of the Prony and NPM see Appendix.

## Empirical Mode Decomposition

Empirical mode decomposition is a data-driven method, which is a powerful tool for non-stationary signal analysis (Huang et al., 1998). This method decomposes a signal into slowly varying time dependent amplitudes and phases components named intrinsic mode functions. The time-frequency decomposition for the input signal is attributed to the Hilbert transform of the intrinsic mode functions extracted by the sifting process(Han and van der Baan, 2013). If $s(t)$ is the input signal, the empirical mode decomposition can be written as:

$$s(t) = \sum_{k=1}^{K} s_k(t) = \sum_{k=1}^{K} A_k(t)\cos(\phi_k(t)), \tag{1}$$

where $A_k(t)$ measures amplitude modulation, and $\phi_k(t)$ measures phase oscillation. Each $s_k(t)$ has a narrow-band waveform and an instantaneous frequency that is smooth and positive. The empirical mode decomposition is powerful, but its mathematical theory is sketchy.

## Prony Method

Prony method extracts damped complex exponential functions (or sinusoids) from a given signal by solving a set of linear equations (Prony, 1795; Lobos et al., 2003; Peter and Plonka, 2013; Mitrofanov and Priimenko, 2015). The Prony method allows for estimation of frequencies, amplitudes and phases of a signal (For details see Appendix). Assume we want to solve the problem:

$$x[n] = \sum_{k=1}^{M} A_k e^{(\alpha_k + j\omega_k)(n-1)\Delta t + j\phi_k}, \tag{2}$$

if let $h_k = A_k e^{j\phi_k}, z_k = e^{(\alpha_k + j\omega_k)\Delta t}$, we derive the concise form

$$x[n] = \sum_{k=1}^{M} h_k z_k^{n-1}. \tag{3}$$

The above M equations can be written in a matrix form:

$$\begin{bmatrix} z_1^0 & z_2^0 & \cdots & z_M^0 \\ z_1^1 & z_2^1 & \cdots & z_M^1 \\ \vdots & \vdots & & \vdots \\ z_1^{M-1} & z_2^{M-1} & \cdots & z_M^{M-1} \end{bmatrix} \begin{bmatrix} h_1 \\ h_2 \\ \vdots \\ h_M \end{bmatrix} = \begin{bmatrix} x[1] \\ x[2] \\ \vdots \\ x[M] \end{bmatrix}. \tag{4}$$

The above $z_k, k = 1, 2, \cdots, M$ of equation 4 can be computed by solving a polynomial of the form:

$$\mathbf{P}(z) = \prod_{k=1}^{M}(z - z_k), \tag{5}$$

equation 5 can also be written in a form:

$$\mathbf{P}(z) = a_0 z^M + a_1 z^{M-1} + \cdots + a_{M-1} z + a_M. \tag{6}$$

The coefficients $a_k$ of the polynomial can be computed by solving the following equation:

$$\sum_{m=0}^{M} a_m x[n-m] = 0. \tag{7}$$

We use the method proposed by Toh and Trefethen (1994) to compute the roots $z_k$ of equation 6. If the roots are solved, the $h_k$ can be computed using equation 3. Finally, the components are computed based on the equation below(For details see Appendix):

$$c_k[n] = h_k z_k^{n-1} = h_k z_k^{n-1}, k = 1, 2, \cdots, M. \tag{8}$$

## Non-stationary Prony method

Equation 7 can be written as:

$$\sum_{m=1}^{M} \hat{a}_m x[n-m] = x[n]. \tag{9}$$

If the $\hat{a}_m$ in equation 9 are time dependent, then we have:

$$\sum_{m=1}^{M} \hat{a}_m[n] x[n-m] \approx x[n], \tag{10}$$

which is an under-determined linear system. There are many methods for solving under-determined linear system, such as Tikhonov method (Tikhonov, 1963). In this paper, we apply shaping regularization (Fomel, 2007, 2009) to regularize the under-determined linear system, and obtain (for details see Appendix):

$$\hat{\mathbf{a}} = \mathbf{F}^{-1}\eta, \tag{11}$$

where $\hat{\mathbf{a}}$ is a vector composed of $\hat{a}_m[n]$, the elements of vector $\eta$ are $\eta_i[n] = \mathbf{S}[x_i^*[n]x[n]]$, where $x_i[n] = x[n-i]$, $x_i^*[n]$ stands for the complex conjugate of $x_i[n]$ and $\mathbf{S}$ is the shaping operator. The elements of matrix $\mathbf{F}$ are:

$$F_{ij}[n] = \sigma^2\delta_{ij} + \mathbf{S}[x_i^*[n]x_j[n] - \sigma^2\delta_{ij}], \tag{12}$$

where $\sigma$ is the regularization parameter. Solving equation 11, we obtain the coefficients vector $\hat{a}_m[n]$ and form a polynomial below:

$$\mathbf{P}(z) = z^M + \hat{a}_1[n] z^{M-1} + \cdots + \hat{a}_M[n]. \tag{13}$$

For the roots computation $\hat{z}_m[n], m = 1, 2, \cdot, M$ of the above polynomial, we use the method proposed by Toh and Trefethen (1994). The instantaneous frequency of each different component is derived from the following equation:

$$f_m[n] = \Re\left[\arg\left(\frac{\hat{z}_m[n]}{2\pi\Delta t}\right)\right]. \tag{14}$$

From the instantaneous frequency, we compute the local phase according to the following equation:

$$\Phi_m[n] = 2\pi \sum_{k=0}^{n} f_m[k]\Delta t. \tag{15}$$

Solving the following equation using regularized non-stationary regression method (Fomel, 2013):

$$x[n] = \sum_{m=1}^{M} \hat{A}_m[n] e^{j\Phi_m[n]} = \sum_{m=1}^{M} c_m[n]. \tag{16}$$

Finally the narrow-band intrinsic mode functions $c_m[n]$ are computed based on equation 16

# EXAMPLES

We use synthetic signals and real field data to test the proposed method.

## Benchmark examples

We use a simple synthetic signal to test the proposed method. Figure 1 is a synthetic signal from Hou and Shi (2013). The three components of the signal are shown in Figure 2. Figure 3 and Figure 4 show the intrinsic mode functions extracted respectively by ensemble empirical mode decomposition and NPM methods. From the figures, we see that the NPM method accurately identifies the three components that the signal has. The intrinsic mode functions derived by the NPM are more smooth with respect to amplitudes and frequencies compared with the intrinsic mode functions obtained by ensemble empirical mode decomposition. For ensemble empirical mode decomposition, we repeat the empirical mode decomposition 25 times with different level of noises to generate the ensemble empirical mode decomposition results. The time-frequency distributions of the input signal are the Hilbert transform of the intrinsic mode functions. Figure 5a, 5b and 5c are respectively the time-frequency distributions using local attribute (Liu et al., 2011), ensemble empirical mode decomposition (Wu and Huang, 2009) and the proposed method for the synthetic signal of Figure 1. Figure 6 is an another synthetic signal. Figure 7a, 7b and 7c are respectively the time-frequency maps using local attribute (Liu et al., 2011), ensemble empirical mode decomposition (Wu and Huang, 2009) and the proposed method. From the figures, we see that the energies compactly spread over the instantaneous

frequencies for the ensemble empirical mode decomposition. However, the energies are not steadily distributed for the ensemble empirical mode decomposition. The proposed method provides a steady and compact energies distribution, which sharpen the time-frequency distribution.

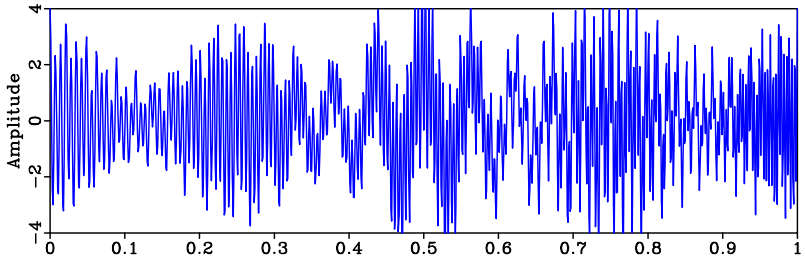


Figure 1: Synthetic signal.

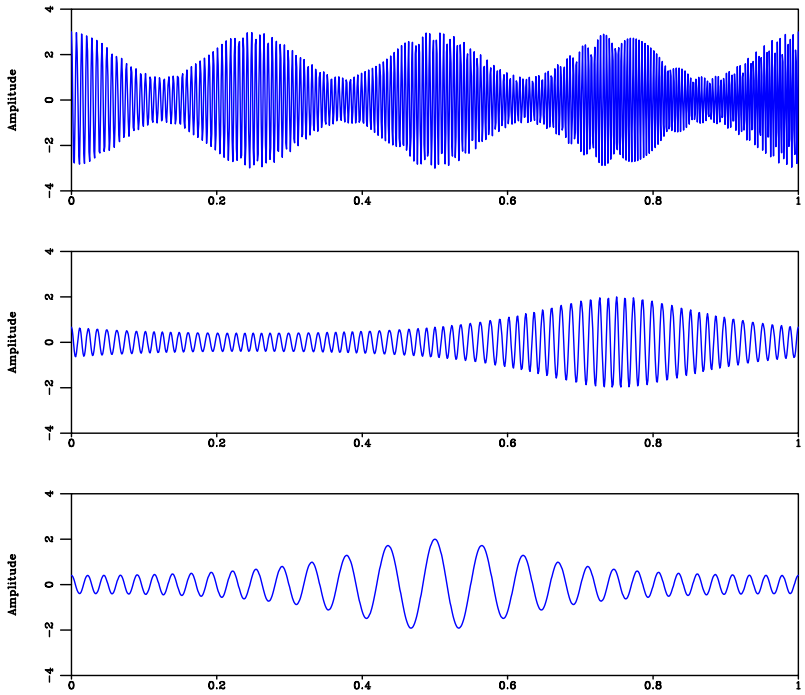


Figure 2: Components of the synthetic signal of Figure 1 .

## Field examples

Figure 8 is a seismic trace from marine survey. Figure 9a, 9b and 9c are the time-frequency distributions of the trace using local attribute (Liu et al., 2011), ensemble empirical mode decomposition and the proposed method. We can see that the energies distributions for ensemble empirical mode decomposition and the proposed method are much like each other. Both the ensemble empirical mode decomposition and

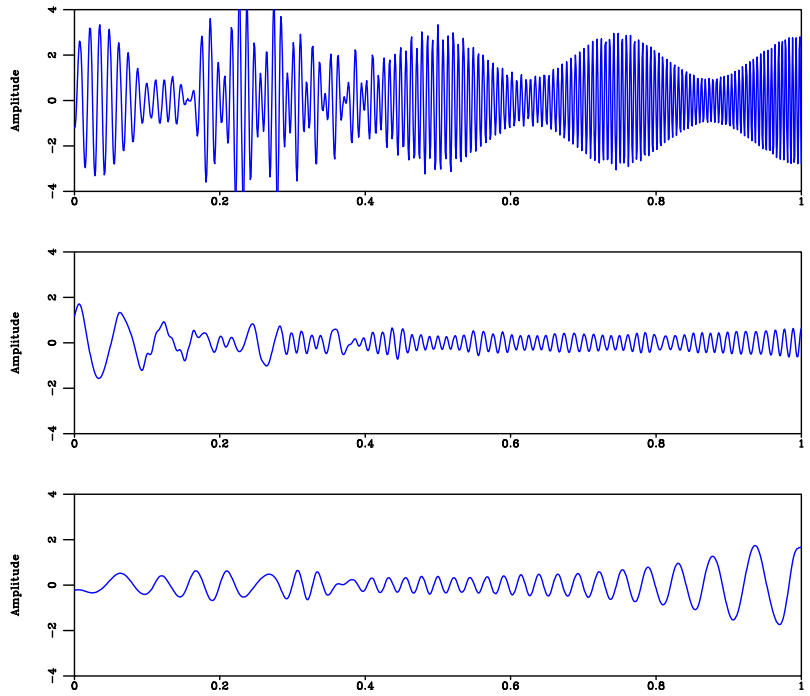


Figure 3: Components of the synthetic signal of Figure 1 using ensemble empirical mode decomposition.

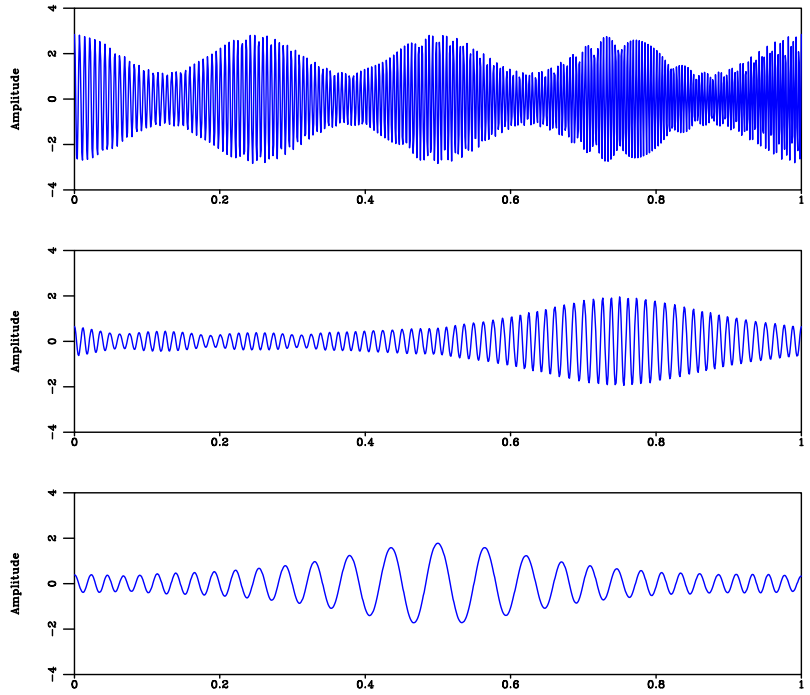


Figure 4: Components of the synthetic signal of Figure 1 using NPM.

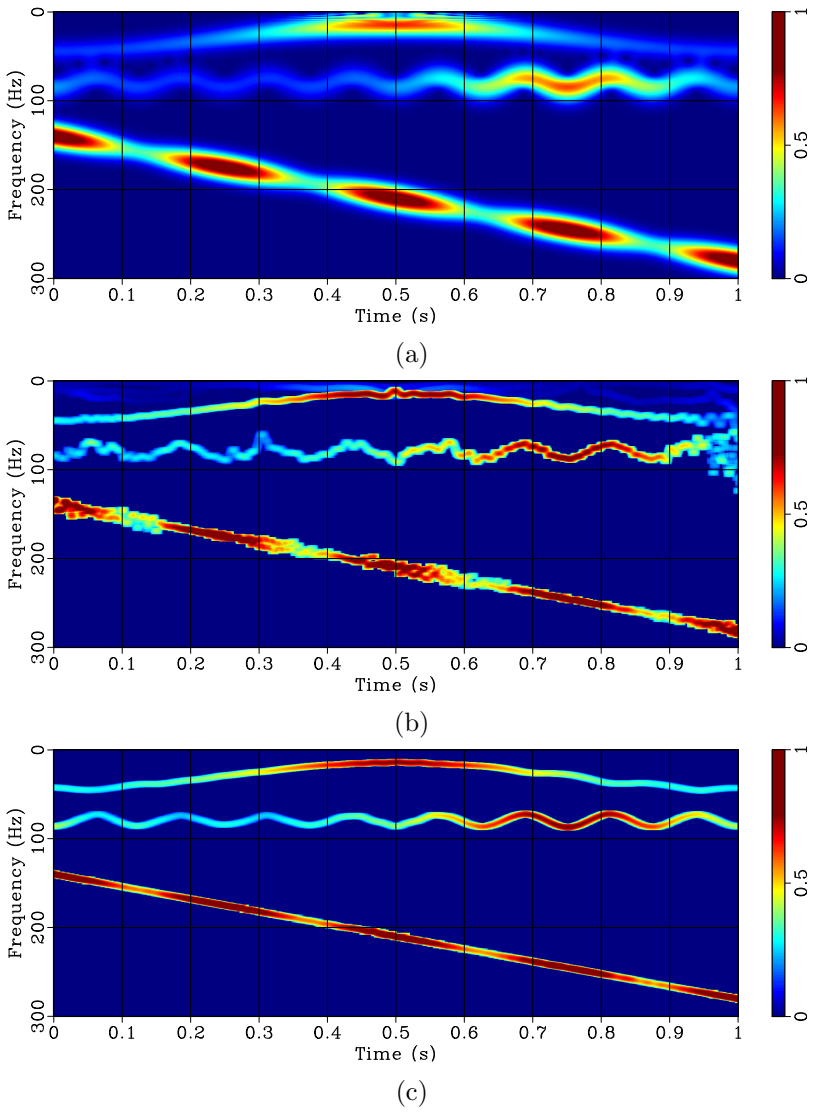


Figure 5: (a) Time-frequency map for synthetic signal of Figure 1 using local attribute. (b) Time-frequency map for synthetic signal of Figure 1 using ensemble empirical mode decomposition. (c) Time-frequency map for synthetic signal of Figure 1 using the proposed method.

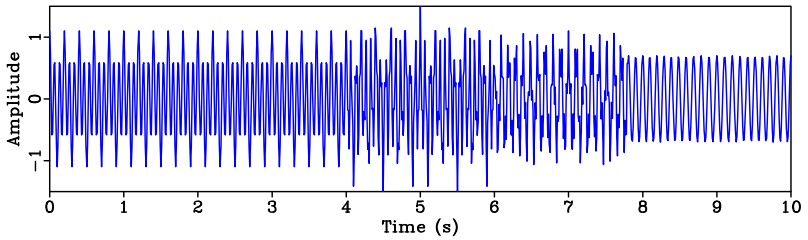


Figure 6: Synthetic signal.

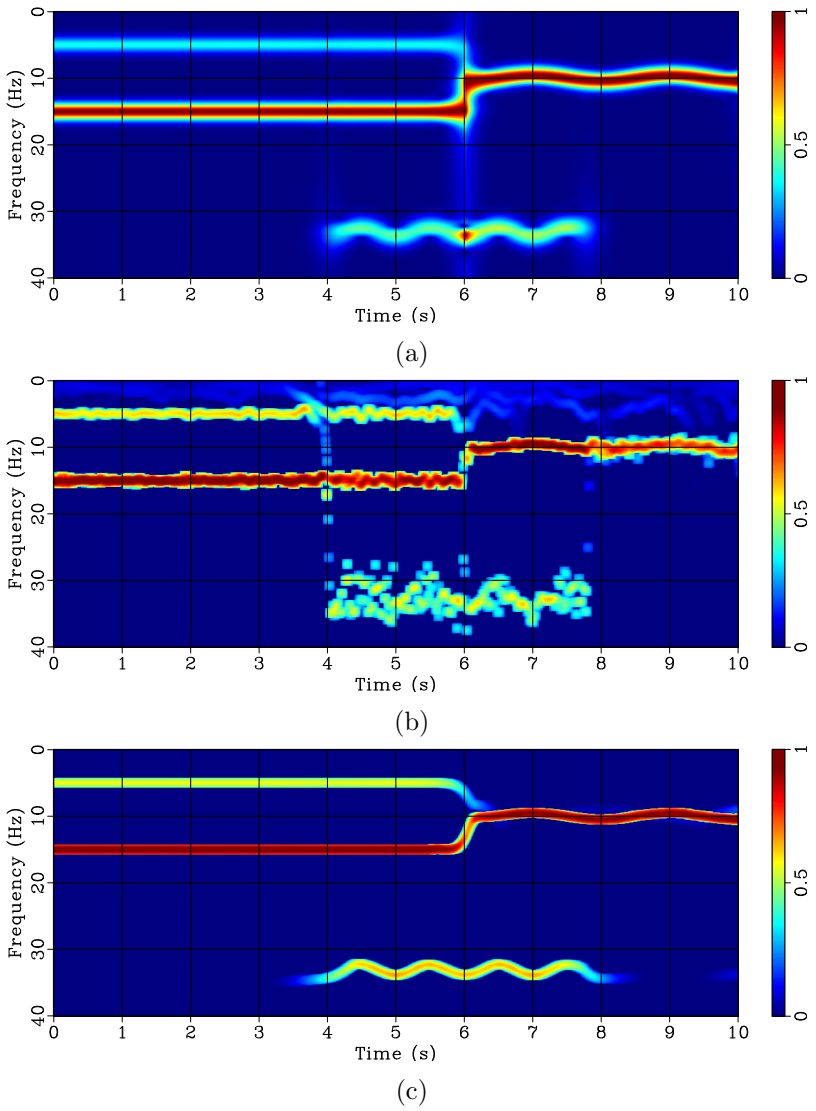


Figure 7: (a) Time-frequency map for synthetic signal of Figure 6 using local attribute. (b) Time-frequency map for synthetic signal of Figure 6 using ensemble empirical mode decomposition. (c) Time-frequency map for synthetic signal of Figure 6 using the proposed method.

the proposed method using the Hilbert transform of the intrinsic mode functions to represent the time-frequency distributions for the input signal. The results confirm that they both reveal the time-frequency character of the input signal.

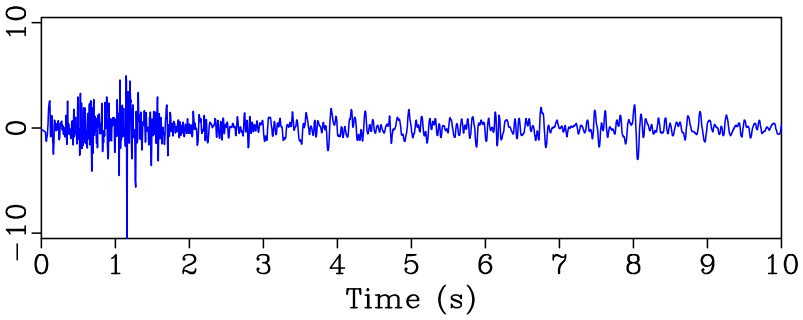


Figure 8: Seismic trace from marine survey.

Low-frequency anomalies are often attributed to abnormally high attenuation in gas-filled reservoirs and can be used as a hydrocarbon indicator (Castagna et al., 2003). The mechanisms of low-frequency anomalies associated with hydrocarbon reservoirs are not clearly understood (Ebrom, 2004; Kazemeini et al., 2009). Figure 10 is a 2D field seismic data. Figure 11a and 11b, 11c and 11d, 11e and 11f are the 30Hz and 60Hz constant frequency slices using local attribute, ensemble empirical mode decomposition and the proposed method. From the above figures, we see that there is a low frequency anomaly in the upper left part of the data section indicated by the text boxes "Gas?" for the ensemble empirical mode decomposition and the proposed methods, which may correspond to gas presentation.

Figure 12a, 12b and 12c are the full time-frequency cubes computed respectively using local attribute, ensemble empirical mode decomposition and the proposed methods. The main panels show constant frequency slices. The right hand side panels show the time-frequency maps of the 150th trace. The top panels show the time-frequency maps of 0.6s time-depth signal. From the right and top side panels we see that there are a lot of noise in the high frequency domain for the ensemble empirical mode decomposition and local attribute methods compared with the proposed method.

## CONCLUSION

We proposed to compute the time-frequency map of an input signal based on NPM coupled with Hilbert spectral analysis. The proposed method is an empirical mode decomposition-like method, but using NPM to compute its intrinsic mode functions. Compared with the Fourier transform, the proposed method is data-driven and needs much less base functions to approximate the original signal. Since the NPM results an under-determined linear system, we use shaping regularization to regularize it. The regularization makes the intrinsic mode functions more smooth with respect to the amplitudes and frequencies compared with the intrinsic mode functions of the

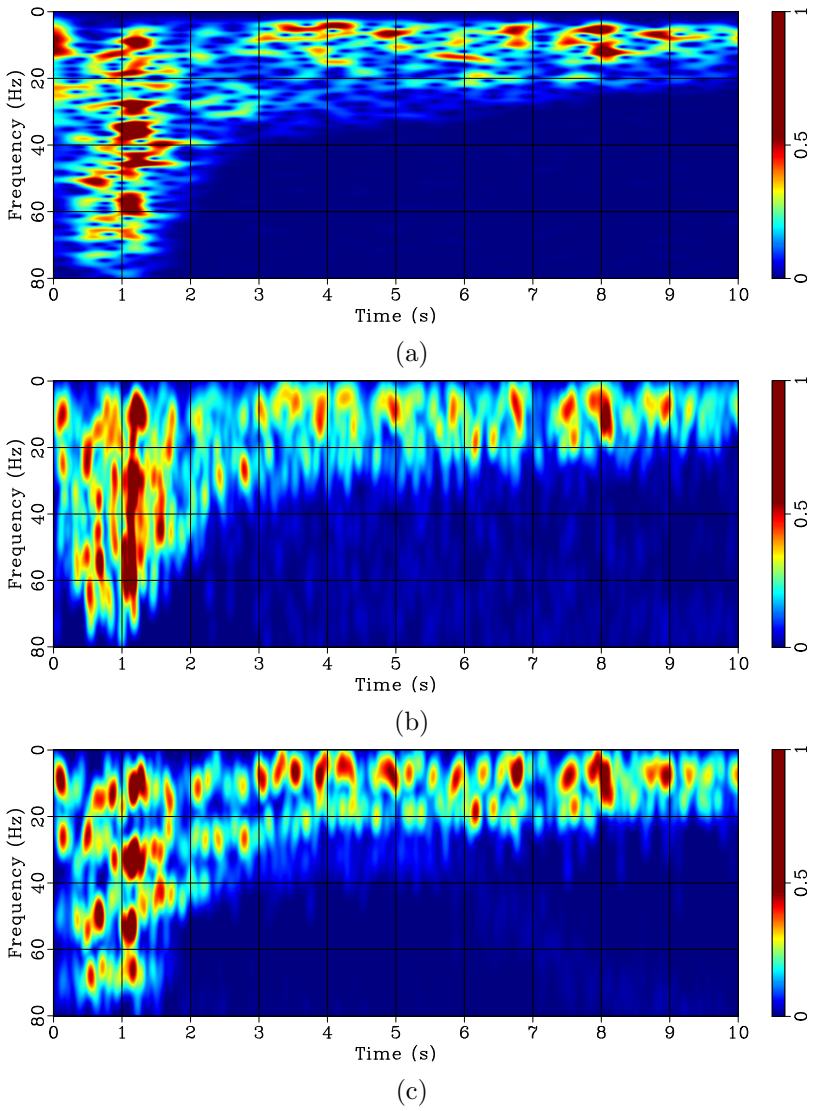


Figure 9: (a) Time-frequency map for synthetic signal of Figure 8 using local attribute. (b) Time-frequency map for synthetic signal of Figure 8 using ensemble empirical mode decomposition. (c) Time-frequency map for synthetic signal of Figure 8 using the proposed method.

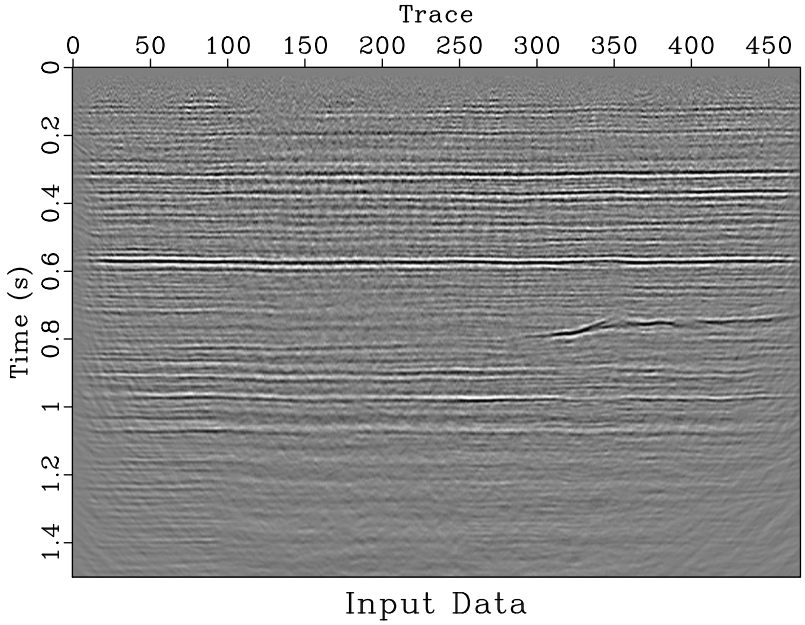


Figure 10: 2D seismic data section.

empirical mode decomposition. There are many time-frequency methods, which one is the best? This is a difficult question to answer. Methods are good for some type signals, maybe not good for other type signals.

Yung-Huang et al. (2014) pointed out that the complexity of empirical mode decomposition/ensemble empirical mode decomposition is $41 * \mathbf{N}_E * \mathbf{N}_S * n(\log_2 n) = O(n \log n)$ , where $n$ is the data length and the parameters $\mathbf{N}_E$ and $\mathbf{N}_S$ are the ensemble and sifting numbers respectively. For the non-stationary Prony method, the computation complexity is mainly attributed to the polynomial zero-finding. We used the pseudo-zeros method to compute the pseudo-spectra of the associated balanced companion matrix (Toh and Trefethen, 1994), which requires approximate $\mathbf{N}^3$ works, where $\mathbf{N}$ is the polynomial degree number. Therefore, the total computation complexity is $\mathbf{N}^3 * \frac{n}{\mathbf{N}} = n * \mathbf{N}^2$, where $n$ is the data length. In this paper, we choose $\mathbf{N} = 5$, and therefore the total computation complexity is approximate $n * 5^2 = O(n)$.

## ACKNOWLEDGMENTS

We would like to thank Zhiguang Xue, and Junzhe Sun for their constructive suggestions. The first author thanks China University of Petroleum-Beijing for supporting his visiting to the Bureau of Economic Geology at UT Austin. The work is partially supported by Youth Science Foundation of China University of Petroleum at Beijing (Grant NO. 01jb0508) and Science Foundation of China University of Petroleum-Beijing (Grant NO.2462015YQ0604).

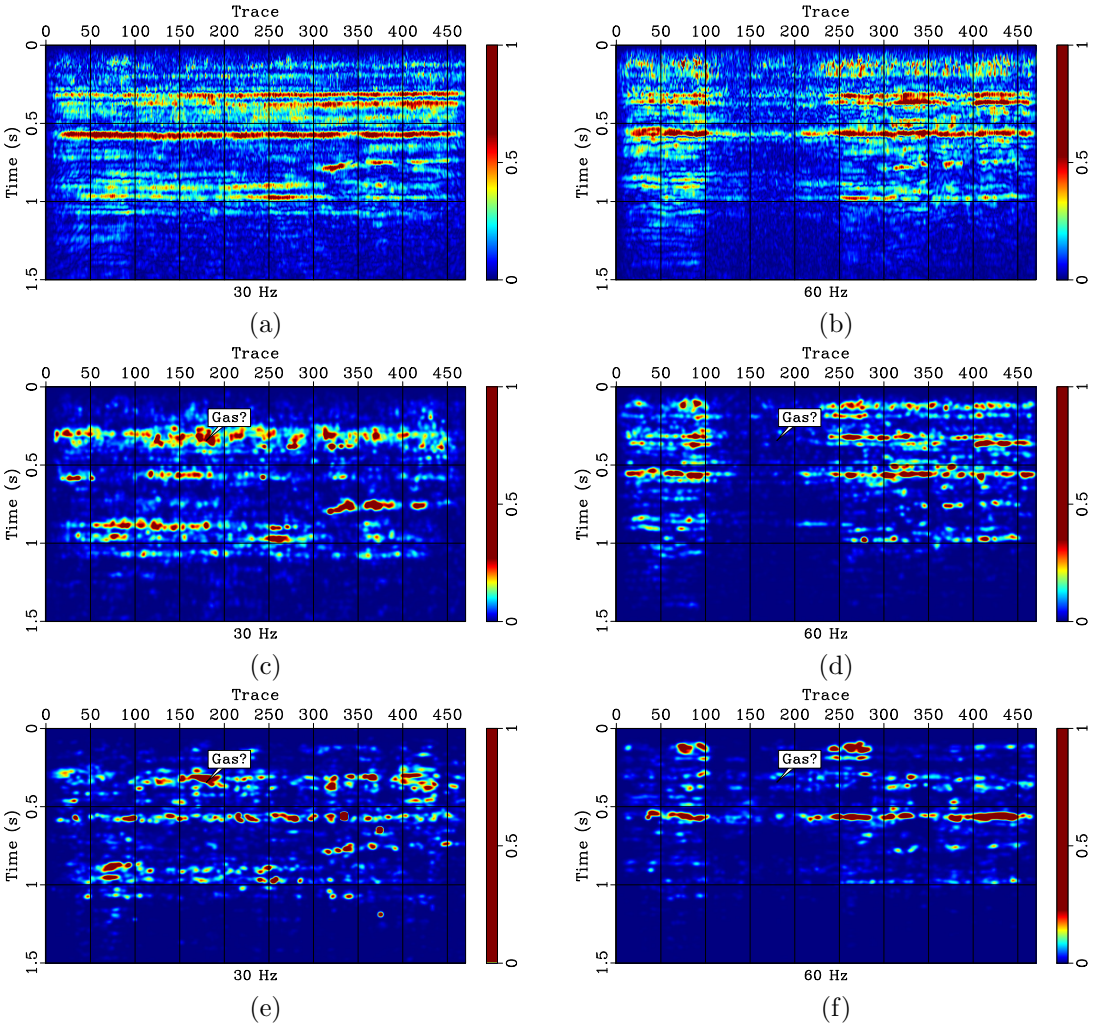


Figure 11: (a) 30Hz slice time-frequency map using local attribute method. (b) 60Hz slice time-frequency map using local attribute method. (c) 30Hz slice time-frequency map using ensemble empirical mode decomposition method. (d) 60Hz slice time-frequency map using ensemble empirical mode decomposition method. (e) 30Hz slice time-frequency map of the proposed method. (f) 60Hz slice time-frequency map of the proposed method.

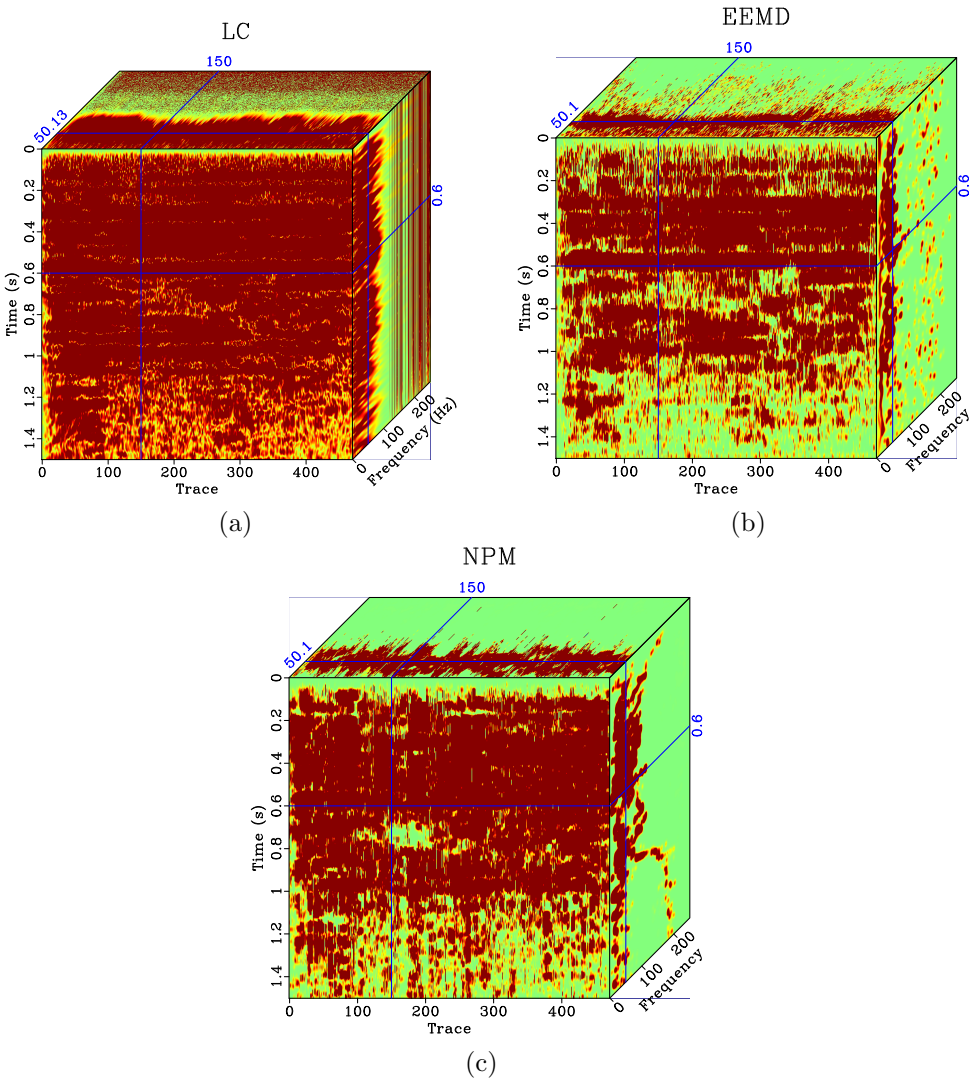


Figure 12: (a) Time-frequency cube using local attribute method. (b) Time-frequency cube using ensemble empirical mode decomposition method. (c) Time-frequency cube using NPM method.

# APPENDIX A: PRONY METHOD

Prony method can extract damped complex exponential signals from a given data by solving a set of linear equations (Prony, 1795; Lobos et al., 2003; Peter and Plonka, 2013; Mitrofanov and Priimenko, 2015). Assume the N complex data samples $x[1], x[2], \cdots x[N]$, we approximate the data by $M$ exponential functions:

$$x[n] \approx \sum_{k=1}^{M} A_k e^{(\alpha_k + j\omega_k)(n-1)\Delta t + j\phi_k}, \tag{17}$$

where $A_k$ is the amplitude, $\Delta t$ is the sampling period, $\alpha_k$ is the damping factor, $\omega_k$ is the angular frequency, $\phi_k$ is the initial phase. If we let $h_k = A_k e^{j\phi_k}, z_k = e^{(\alpha_k + j\omega_k)\Delta t}$, we then derive the concise form below:

$$x[n] \approx \sum_{k=1}^{M} h_k z_k^{n-1}. \tag{18}$$

The approximation problem above can be solved based on the error minimization:

$$\mathbf{min} \sum_{n=1}^{N} |\epsilon[n]|^2 = \mathbf{min} \sum_{n=1}^{N} \left| x[n] - \sum_{k=1}^{M} h_k z_k^{n-1} \right|^2. \tag{19}$$

This turns to be a nonlinear problem. It can be solved using Prony method that utilizes linear equation solutions. If there are as many data samples as parameters of the approximation problem, the above M equations **18** can be expressed:

$$x[n] = \sum_{k=1}^{M} h_k z_k^{n-1}. \tag{20}$$

**20** can be written in a matrix form as below:

$$\begin{bmatrix} z_1^0 & z_2^0 & \cdots & z_M^0 \\ z_1^1 & z_2^1 & \cdots & z_M^1 \\ \vdots & \vdots & & \vdots \\ z_1^{M-1} & z_2^{M-1} & \cdots & z_M^{M-1} \end{bmatrix} \begin{bmatrix} h_1 \\ h_2 \\ \vdots \\ h_M \end{bmatrix} = \begin{bmatrix} x[1] \\ x[2] \\ \vdots \\ x[M] \end{bmatrix}. \tag{21}$$

Prony proposed to define the polynomial that has the above $z_k, k = 1, 2, \cdots, M$ as its roots (Prony, 1795):

$$\mathbf{P}(z) = \prod_{k=1}^{M} (z - z_k). \tag{22}$$

Equation **22** can be rewritten in the form below:

$$\mathbf{P}(z) = a_0 z^M + a_1 z^{M-1} + \cdots + a_{M-1} z + a_M. \tag{23}$$

Shifting the index on equation **20** from $n$ to $n-m$ , and multiplying by parameter $a[m]$, then we derive:

$$\sum_{m=0}^{M} a_m x[n-m] = \sum_{k=1}^{M} h_k z_k^{n-M-1} \sum_{m=0}^{M} a[m] z_k^{M-m}. \tag{24}$$

Notice $z_k, k = 1, 2, \cdots, M$ are roots of equation **23**, then equation **24** be written as:

$$\sum_{m=0}^{M} a_m x[n-m] = 0. \tag{25}$$

Solving equation **25** for the polynomial coefficients. In subsequent steps we compute the frequencies, damping factors and the phases according to Algorithm 1. After all the parameters are computed, we then compute the components of the input signal. For details see Algorithm 1 as follows:

ALGORITHM 1: PRONY METHOD()

Find coefficients:

$a_k, k = 1, 2, \cdots, M \leftarrow \sum_{m=0}^{M} a_m x[n-m] = 0.$

Find roots: $z_k, k = 1, 2, \cdots, M \leftarrow \sum_{m=0}^{M} a_m z^{M-m} = 0.$

Compute frequencies:

$\omega_k, k = 1, 2, \cdots, M \leftarrow \Re\left\{ \mathbf{arg}\left( \frac{z_k}{(k-1)\Delta t} \right) \right\}, k = 1, 2, \cdots, M.$

Compute:

$A_k e^{\alpha_k (n-1)\Delta t + j\phi_k}, k = 1, 2, \cdots, M \leftarrow$

$x[n] = \sum_{k=1}^{M} A_k e^{(\alpha_k + j\omega_k)(n-1)\Delta t + j\phi_k}.$

Compute components:

$A_k e^{(\alpha_k + j\omega_k)(n-1)\Delta t + j\phi_k}.$

## APPENDIX B: NON-STATIONARY PRONY METHOD AND SHAPING REGULARIZATION

The equation **25** can be rewritten as

$$\sum_{m=1}^{M} \hat{a}_m x[n-m] = x[n]. \tag{26}$$

If the $\hat{a}_m, m = 1, 2, \cdots, M$ in equation **26** are time dependent, then we have

$$\sum_{m=1}^{M} \hat{a}_m[n] x[n-m] \approx x[n], \tag{27}$$

which is under-determined. There many methods for the solving under-determined linear system. For example, Tikhonov (1963) used the regularization method for making the under-determined problem well-posed by adding constraints on the estimated model.

## Shaping regularization

Fomel (2007, 2009) introduces shaping regularization in inversion problem, which regularizes the under-determined linear system by mapping the model to the space of acceptable models. Consider a linear system given as $\mathbf{Fx} = \mathbf{b}$, where $\mathbf{F}$ is the forward-modeling map, $\mathbf{x}$ is the model vector, and $\mathbf{b}$ is the data vector. Tikhonov regularization method amounts to minimize the least square problem bellow (Tikhonov, 1963):

$$\mathbf{min}\|\mathbf{Fx} - \mathbf{b}\|^2 + \epsilon^2\|\mathbf{Dx}\|^2, \tag{28}$$

where $\mathbf{D}$ is the regularization operator, and $\epsilon$ is a scalar parameter. The solution for equation **28** is:

$$\hat{\mathbf{x}} = \left(\mathbf{F}^T\mathbf{F} + \epsilon^2\mathbf{D}^T\mathbf{D}\right)^{-1}\mathbf{F}^T\mathbf{b}, \tag{29}$$

Where $\hat{\mathbf{x}}$ is the least square approximated of $\mathbf{x}$, $\mathbf{F}^T$ is the adjoint operator. If the forward operator $\mathbf{F}$ is simply the identity operator, the solution of equation **29** is the form below:

$$\hat{\mathbf{x}} = \left(\mathbf{I} + \epsilon^2\mathbf{D}^T\mathbf{D}\right)^{-1}\mathbf{b}, \tag{30}$$

which can be viewed as a smoothing process. If we let:

$$\mathbf{S} = \left(\mathbf{I} + \epsilon^2\mathbf{D}^T\mathbf{D}\right)^{-1}, \tag{31}$$

or

$$\epsilon^2\mathbf{D}^T\mathbf{D} = \mathbf{S}^{-1} - \mathbf{I}. \tag{32}$$

Substituting equation **32** into equation **29** yields a solution by shaping regularization:

$$\hat{\mathbf{x}} = \left(\mathbf{F}^T\mathbf{F} + \mathbf{S}^{-1} - \mathbf{I}\right)^{-1}\mathbf{F}^T\mathbf{b} = \left[\mathbf{I} + \mathbf{S}\left(\mathbf{F}^T\mathbf{F} - \mathbf{I}\right)\right]^{-1}\mathbf{S}\mathbf{F}^T\mathbf{b}. \tag{33}$$

The forward operator $\mathbf{F}$ may has physical units that require scaling. Introducing scaling $\lambda$ into $\mathbf{F}$, equation **33** be written as:

$$\hat{\mathbf{x}} = \left[\lambda^2\mathbf{I} + \mathbf{S}\left(\mathbf{F}^T\mathbf{F} - \lambda^2\mathbf{I}\right)\right]^{-1}\mathbf{S}\mathbf{F}^T\mathbf{b}. \tag{34}$$

If $\mathbf{S} = \mathbf{H}\mathbf{H}^T$ with square and invertible $\mathbf{H}$. Equation **34** can be written as:

$$\hat{\mathbf{x}} = \mathbf{H}\left[\lambda^2\mathbf{I} + \mathbf{H}^T\left(\mathbf{F}^T\mathbf{F} - \lambda^2\mathbf{I}\right)\mathbf{H}\right]^{-1}\mathbf{H}^T\mathbf{F}^T\mathbf{b}. \tag{35}$$

The conjugate gradient algorithm can be used for the solution of the equation **35**.

## Non-stationary Prony method

Equation **27** can be written as a matrix form:

$$\sum_{m=1}^{M} \hat{\mathbf{a}}_m(t)\mathbf{x}_m(t) \approx \mathbf{d}(t), \tag{36}$$

where $\mathbf{d}(t) = \mathbf{x}(t)$, $\mathbf{x}_m(t) = \mathbf{x}(t - m\Delta t)$ is the time shift of the input signal $\mathbf{x}(t)$ and $\hat{\mathbf{a}}_m(t)$ is the time-dependant coefficients. We solve the under-determined linear system by using the shaping regularization method. The solution is the form below:

$$\mathbf{a} = \mathbf{F}^{-\mathbf{1}}\eta, \tag{37}$$

where $\mathbf{a}$ is a vector of $\hat{a}(t)$, the elements of vector $\eta$ is:

$$\eta_i(t) = \mathbf{S}\left[\mathbf{x}_i^*(t)\mathbf{d}(t)\right], \tag{38}$$

the elements of the matrix $\mathbf{F}$ is:

$$\mathbf{F}_{ij} = \sigma^2\delta_{ij} + S[\mathbf{x}_i^*(t)\mathbf{x}_j(t) - \sigma^2\delta_{ij}] \tag{39}$$

where $\sigma$ is the regularization parameter, $\mathbf{S}$ is a shaping operator, and $\mathbf{x}_i^*(t)$ stands for the complex conjugate of $\mathbf{x}_i(t)$. We can use the conjugate gradient method to find the solution of the linear system. The NPM (Fomel, 2013) can be summarized as follows:

Algorithm 2: non-stationary Prony method()

1 Find time dependent coefficients using auto-regression method:

2 $\hat{a}_k[n], k = 1, \cdots, M \leftarrow \sum_{m=0}^{M} \hat{a}_m[n]x[n-m] = 0.$

3 Find time dependent roots:

4 $\hat{z}_k[n], k = 1, 2, \cdots, M \leftarrow \sum_{m=0}^{M} \hat{a}_m[n]z^{M-m} = 0.$

5 Compute time dependent frequencies:

6 $\hat{\omega}_k[n], k = 1, \cdots, M \leftarrow \Re\left\{\mathbf{arg}\left(\frac{\hat{z}_k[n]}{\Delta t}\right)\right\}, k = 1, \cdots, M.$

7 Compute the time dependent phase:

8 $\hat{\phi}_k[n] = \sum_{k=0}^{n} \hat{\omega}_k[n]\Delta t.$

9 Compute components using auto-regression method:

10 $\hat{c}_m[n], m = 1, \cdots M \leftarrow \mathbf{x}[n] \approx \sum_{m=1}^{M} \hat{A}_m[n]e^{j\hat{\phi}_m[n]} = \sum_{m=1}^{M} \hat{c}_m[n]$

After we decompose the input signal into narrow-band components, we compute the time-frequency distribution of the input signal using the Hilbert transform of the intrinsic mode functions.

## REFERENCES

Castagna, J., S. Sun, and R. W. Siegfried, 2003, Instantaneous spectral analysis: Detection of low-frequency shadows associated with hydrocarbons: The Leading Edge, **22**, 120–127.

Chen, S. S., D. L. Donoho, and M. A. Saunders, 1998, Atomic decompositon by basis pursuit: Society for industrial and applied mathematics, **20**, 33–61.

Chen, Y., and S. Fomel, 2015, EMD-seislet transform: 85th Annual International Meeting, SEG, Expanded Abstracts, 4775–4778.

Chen, Y., T. Liu, X. Chen, J. Li, and E. Wang, 2014, Time-frequency analysis of seismic data using synchrosqueezing wavelet transform: Journal of Seismic Exploration, **23**, 303–312.

Cohen, L., 1989, Time-frequency distributions – A review: Proceedings of the IEEE, **77**, 941–981.

Daubechies, I., J. Lu, and H. T. Wu, 2011, Synchrosqueezed wavelet transforms: An empirical mode decomposition-like tool: Applied and Computational Harmonic Analysis, **30**, 243–261.

Ebrom, D., 2004, The low frequency gas shadows in seismic sections: The Leading Edge, **23**, 772.

Fomel, S., 2007, Shaping regularization in geophysical-estimation problems: Geophysics, **72**, R29–R36.

———, 2009, Adaptive multiple subtraction using regularized nonstationary regression: Geophysics, **74**, V25–V33.

———, 2013, Seismic data decomposition into spectral components using regularized nonstationary autoregression: Geophysics, **78**.

Han, J., and M. van der Baan, 2013, Empirical mode decomposition for seismic time-frequency analysis: Geophysics, **78**, O9–O19.

Hou, T. Y., and Z. Shi, 2013, Data-driven time-frequency analysis: Applied and Computational Harmonic Analysis, **35**, 284–308.

Huang, N. E., Z. Shen, S. R. Long, M. C. Wu, H. H. Shih, Q. Zheng, N.-C. Yen, C. C. Tung, and H. H. Liu, 1998, The empirical mode decomposition and the Hilbert spectrum for nonlinear and non-stationary time series analysis: Proceeding of the Royal Society of London Series A, **454**, 903–995.

Huang, Z., J. Zhang, T. hu Zhao, and Y. Sun, 2015, Synchrosqueezing s-transform and its application in seismic spectral decomposition: IEEE Transactions on Geoscience and Remote Sensing, **54**, 817–825.

Kazemeini, S. H., C. Juhlin, K. Z. Jorgensen, and B. Norden, 2009, Application of the continuous wavelet transform on seismic data for mapping of channel deposits and gas detection at the CO2SINK site, Ketzin, Germany: Geophysical Prospecting, **57**, 111–123.

Liu, G., S. Fomel, and X. Chen, 2011, Time-frequency analysis of seismic data using local attributes: Geophysics, **76**, P23–P34.

Liu, W., S. Cao, and Y. Chen, 2016, Seismic time-frequency analysis via empirical wavelet transform: IEEE Geoscience and Remote Sensing Letters, **13**, 28–32.

Lobos, T., J.Rezmer, and J. Schegner, 2003, Parameter estimation of distorted signals

using prony method: Power Tech Conference Proceedings, 41–44.

Mallat, S., 2009, A wavelet tour of signal processing: The sparse way: Academic Press.

Mallat, S., and Z. Zhang, 1993, Matching pursuit with time-frequency dictionaries: IEEE Transactions on Signal Processing, **41**, 3397–3415.

Mallat, S. G., 1989, A theory for multiresolution signal decomposition: The wavelet representation: IEEE Trans. Pattern Anal. Mach. Intell., **11**, 674–693.

Mitrofanov, G., and V. Priimenko, 2015, Prony filtering of seismic data: Acta Geophys., **63**, 652–678.

Oberlin, T., S. Meignen, and V. Perrier, 2014, The fourier-based synchrosqueezing transform: Proc. IEEE int. Conf. Acoust. Speech Signal Process, 315–319.

Peter, T., and G. Plonka, 2013, A generalized prony method for reconstruction of sparse sums of eigenfunctions of linear operators: Inverse Problems, **29**, 025001.

Prony, R., 1795, Essai expérimental et analytique: Annuaire de l'École Polytechnique, **1**, 24.

Reine, C., M. van der Baan, and R. Clark, 2009, The robustness of seismic attenuation measurements using fixed- and variable-window time-frequency transforms: Geophysics, **74**, 123–135.

Stockwell, R. G., L. Mansinha, and R. P. Lowe, 1996, Localization of the complex spectrum: IEEE Transactions on Signal Processing, **44**, 998–1001.

Tary, J. B., R. H. Herrera, J. Han, and M. van der Baan, 2014, Spectral estimation-what is new? what is next?: Reviews of Geophysics, **52**, 723–749.

Tikhonov, A. N., 1963, Solution of incorrectly formulated problems and the regularization method: Sovet Math. Dokl., 1035–1038.

Toh, K., and L. Trefethen, 1994, Pseudozeros of polynomials and pseudospectra of companion matrices: Mathematik, **68**, 403–425.

Torres, M. E., M. A. Colominas, G. Schlotthauer, and P. Flandrin, 2011, A complete ensemble empirical mode decomposition with adaptive noise: IEEE International Conference on Acoustics, Speech and Signal Processing (ICASSP), IEEE, 4144–4147. (ISBN: 978-1-4577-0538-0 ISSN:1520-6149).

Wu, Z., and N. E. Huang, 2009, Ensemble empirical mode decomposition: a noise-assisted data analysis method: Advances in Adaptive Data Analysis, **1**, 1–41.

Yung-Huang, W., Y. Chien-Hung, Y. H. wen Vincent, H. Kun, and L. Men-Tzung, 2014, On the computational complexity of the empirical mode decomposition algorithm: Physica A: Statistical Mechanics and its Applications, **400**, 159–167.